

UNCLASSIFIED

AD 266 790

*Reproduced  
by the*

ARMED SERVICES TECHNICAL INFORMATION AGENCY  
ARLINGTON HALL STATION  
ARLINGTON 12, VIRGINIA



20050204 154

UNCLASSIFIED

Best Available Copy

NOTICE: When government or other drawings, specifications or other data are used for any purpose other than in connection with a definitely related government procurement operation, the U. S. Government thereby incurs no responsibility, nor any obligation whatsoever; and the fact that the Government may have formulated, furnished, or in any way supplied the said drawings, specifications, or other data is not to be regarded by implication or otherwise as in any manner licensing the holder or any other person or corporation, or conveying any rights or permission to manufacture, use or sell any patented invention that may in any way be related thereto.

100-400000

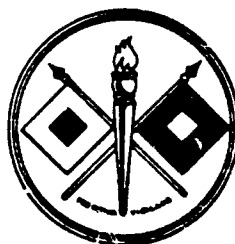
AD NO. \_\_\_\_\_  
ASTIA FILE COPY 266790

XEROX  
USASRD Technical Report 2231

10

# RADIATION FROM PLANET EARTH

by  
I. L. Goldberg



September 1961

U.S. ARMY SIGNAL RESEARCH AND DEVELOPMENT LABORATORY  
FORT MONMOUTH, N. J.



U. S. ARMY SIGNAL RESEARCH AND DEVELOPMENT LABORATORY  
FORT MONMOUTH, NEW JERSEY

September 1961

USASRD L Technical Report 9231 has been prepared under the supervision of the Director Surveillance Department, and is published for the information and guidance of all concerned. Suggestions or criticisms relative to the form, contents, purpose, or use of this publication should be referred to the Commanding Officer, U. S. Army Signal Research and Development Laboratory, Fort Monmouth, New Jersey, ATTN: Chief, Reconnaissance Branch, Applied Physics Division.

J. M. KIMBROUGH, JR.  
Colonel Signal Corps  
Commanding

OFFICIAL:  
Adjutant

DISTRIBUTION:  
Special

ASTIA Availability Notice

Qualified requestors may obtain copies of  
this report from ASTIA.

September 1961

USASRD Technical Report 2231

RADIATION FROM PLANET EARTH

I. L. Goldberg

DA TASK NR. 3A99-23-001-04

U. S. ARMY SIGNAL RESEARCH AND DEVELOPMENT LABORATORY

FORT MONMOUTH, NEW JERSEY

#### ABSTRACT

Information is given on the part played by the sun, earth's surface, and atmosphere in the heat balance of our planet. Following a general survey of solar and terrestrial radiation, including the emissivity and reflectivity of various terrestrial features (clouds, land masses, oceans), an estimate is made of the planetary radiation received by a satellite radiometer in five spectral channels covering the ultraviolet, visible, and infrared spectral regions. The wavelengths and purpose for selecting each of the channels is given below:

- |     |             |         |                                 |
|-----|-------------|---------|---------------------------------|
| (1) | 0.2 - 5.5   | microns | (total albedo of the earth)     |
| (2) | 8 - 30      | microns | (total emission from the earth) |
| (3) | 8 - 12      | microns | (surface and cloud emission)    |
| (4) | 0.55 - 0.75 | microns | (cloud cover)                   |
| (5) | 5.5 - 6.9   | microns | (tropopause temperature)        |

The signal-to-noise ratios associated with the received radiation in each channel, using bolometers such as those in TIROS II and III, are ~~also~~ included.

## CONTENTS

Abstract	1
INTRODUCTION	1
DISCUSSION	1
Heat Balance of the Earth	1
Solar Radiation and Reflection	3
Terrestrial Radiation	11
Radiation in Five Spectral Regions	14
S/N Calculations	22
SUMMARY	24
REFERENCES	25
APPENDICES	
1. Optical Air Mass	27
2. Average Transmission through a Planetary Atmosphere	29
3. Satellite Detector Look Angle and Zenith Angle	33
4. Latent Heat Transfer Due to Evaporation	35

## FIGURES

1. Solar and Terrestrial Radiation	7
2. Depletion of Solar Radiation	9
3. Terrestrial Radiation to Space as a Function of Latitude	12
4. Apparent Radiation in the 8 - 13 Micron Region vs Detector Zenith Angle for Various Surface Temperatures when $q_0$ is Equal to .75	18
5. $N_a$ vs $\phi$ in the 8 - 13 Micron Region for $q_0$ Equal to .85.	19
6. Geometry for Calculating Average Transmission of a Planetary Atmosphere	30
7. Detector Look Angle Geometry	33
8. Zenith Angle $\theta$ vs Look Angle $\theta'$ for Various Detector Altitudes $h$	34

## TABLES

1. Heat Budget of the Earth	4
2. Infrared Atmospheric Absorption Bands	8
3. Albedos of Various Earth Features	10
4. Cloud Albedos	11
5. Emissivities of Various Terrestrial Features	13
6. Apparent Radiance Values of Various Earth Surface Features	16
7. Maximum Value of S/N for Each Channel	24
8. Optical Air Mass as a Function of Zenith Angle	28
9. Values of the Exponential Integral	32

## RADIATION FROM PLANET EARTH

### INTRODUCTION

The advent of artificial earth satellites has made possible the detailed, direct, rapid, and wide coverage measurement of terrestrial and reflected solar radiation to space. A suitable radiometer orbiting the earth can be used to determine such phenomena as the albedo of various portions of the earth's surface and clouds, the self-emission of the earth's surface and atmosphere, cloud cover, and tropopause temperatures. To do this the radiation received by the satellite radiometer must be divided into different spectral regions. We shall divide the radiation into five regions or channels with a separate detector (bolometer) for each channel as was done for the radiometer used in TIROS II.<sup>1</sup> The wavelength ranges and immediate purpose of each channel is listed below.

- |     |             |         |                          |
|-----|-------------|---------|--------------------------|
| (1) | 0.2 - 5.5   | microns | (total earth albedo)     |
| (2) | 8 - 30      | microns | (total emission)         |
| (3) | 8 - 12      | microns | (surface cloud emission) |
| (4) | 0.55 - 0.75 | microns | (cloud cover)            |
| (5) | 5.5 - 6.9   | microns | (tropopause temperature) |

The reason for using these spectral regions for the purposes mentioned is explained in the discussion.

To intelligently interpret the wealth of information anticipated by such satellite radiometers it is essential to understand the contributions made by the sun, earth's surface, and atmosphere in the five spectral regions through which the radiometer receives the radiation. This report will supply both general information on solar and terrestrial radiation and details on the amount of radiation which should be received in each of the five spectral regions.

### DISCUSSION

#### Heat Balance of the Earth

As is well known, the sun is the primary source of energy for the earth. Our planet receives a continuous supply of  $1.6 \times 10^{17}$  watts of power from the sun. Of this amount 65% is absorbed by the earth's surface and atmosphere; the remaining 35% is reflected back to space. The solar irradiation at normal incidence just outside the atmosphere at the mean solar distance (92,900,000 miles) is called the solar constant,<sup>2</sup> and is 0.140 watts/cm<sup>2</sup> or 2.00 cal/cm<sup>2</sup>/minute. The varying solar distance throughout the year causes the irradiation to change by as much as 3.5% from the mean. Solar activity can produce fluctuations of 1.5% in the solar constant. In addition to these relatively small variations, the amount of solar radiation that reaches a particular portion of the earth's surface varies with the solar angle of elevation and atmospheric conditions.



If the atmosphere were completely transparent to solar radiation the irradiation  $H$  on a horizontal element of area on the earth's surface could be expressed as

$$H = \frac{r_m^2}{r^2} S \cos \theta, \quad (1)$$

where

$r_m$  = mean earth-sun distance

$r$  = actual earth-sun distance

$\theta$  = solar zenith angle (complement of solar elevation angle)

$S$  = solar constant.

For a completely transparent atmosphere the region with the largest midday irradiation would not necessarily receive the largest amount of energy over the course of a day. In fact, at the summer solstice in the north latitudes the North Pole with its 24 hours of daylight would receive the maximum daily insolation.\* This is not actually the case, however, since the atmosphere is less transparent to solar radiation at larger zenith angles. This subject is discussed further in the next section.

The spectral distribution of solar radiation resembles that of a blackbody at 5800°K. Over 99% of solar radiation is contained in the wavelength region between 0.2 and 5.5 microns. The earth's surface radiates like a blackbody also, but at a much lower temperature (between about 220°K and 320°K depending on the geographical location at the time). Even at a temperature of 320°K, less than 4% of the earth's surface radiation lies below 5.5 microns. In addition, some of this radiation is absorbed by the atmosphere. The atmosphere emits radiation to space almost like a blackbody at temperatures which are generally lower than that of the surface. It is therefore not difficult to distinguish between terrestrial and reflected solar radiation.

The atmosphere plays a dominant role in the energy which is radiated to space because of its scattering, reflecting (by clouds), radiating, and selective absorption properties. It absorbs about 17% and scatters or reflects out about 31% of solar radiation. An additional 4% is reflected back to space by the earth's surface. Of the outgoing terrestrial radiation (to space), 86% comes from the atmosphere; 14% comes directly from the earth's surface. These are average figures for the earth as a

\*Insolation is defined as the solar irradiation at the earth's surface, including both direct and scattered radiation. Daily insolation is the total solar energy received per unit horizontal area over the course of 24 hours.

whole, assuming a mean cloud cover of 5-6%. The major atmospheric absorber of infrared radiation is water vapor. Carbon dioxide and, to a lesser extent, ozone also absorb in the infrared region. Although there are many other atmospheric absorbers they are relatively unimportant for our purposes here.

In the absence of clouds, the atmosphere transmits radiation in certain spectral regions with little absorption. These regions are called atmospheric windows and will be discussed in more detail later. Even when no clouds are present the atmosphere is opaque to surface radiation except in the 8-13 micron window. Within this window there exists a strong but narrow ozone absorption band which does not radically change the total amount of energy passing through.

A summary of the heat budget of the earth is given in Table 1. The incoming solar radiation which is averaged over the entire surface of the earth is  $35.0 \text{ mW/cm}^2$  or  $S/4$ .\* From the table it can be seen that the earth's surface emits more radiation than the earth receives from the sun. However, most of the surface radiation is absorbed by the atmosphere and reradiated back, similar to the action of glass in a greenhouse which passes solar radiation but is opaque to the long-wave earth radiation.

The value for evaporation shown in Table 1 is based on a global mean precipitation of 100 cm per year. The method of computation is shown in Appendix 4. The value listed for eddy currents was found indirectly by equating the total outgoing and incoming (absorbed) surface radiation. Some of the long-wave atmospheric radiation striking the earth's surface is reflected back (the earth has a mean absorptivity of .93 in the long wave region). However, nearly all of this reflected radiation is absorbed by the atmosphere. The atmospheric radiation to the earth's surface shown in the table is the net value. The other values shown in Table 1 are discussed in greater detail in the following sections.

### Solar Radiation and Reflection

#### 1. Variation of Insolation with Latitude

The direct solar spectral irradiation (power per unit wavelength per unit area) on a horizontal portion of the earth's surface when the sun is directly overhead ( $\theta = 0$ ) can be expressed by

$$E_{\lambda}(0) d\lambda = \frac{r_E^2}{r^2} S_{\lambda} q_{\lambda 0} d\lambda, \quad (2)$$

\*If  $r$  is the radius of the earth, then the solar radiation intercepted by the earth is  $\pi r^2 S$ . Since the surface area of the earth is  $4\pi r^2$  the average solar irradiation, taken over the earth's surface is

$$\frac{\pi r^2 S}{4\pi r^2} = \frac{S}{4}$$

TABLE I  
HEAT BUDGET OF THE EARTH

PLANETARY BALANCE

AVERAGE INCOMING RADIATION

35.0  $\text{mw/cm}^2$

PLANETARY RADIATION TO SPACE

Scattered or reflected by atmosphere	10.9
Reflected by surface	1.3
Direct radiation by surface	3.2
Radiated by troposphere	18.6
Radiated by stratosphere	1.0
	<u>35.0</u>

SURFACE BALANCE

RADIATION ABSORBED BY SURFACE VIA

Direct Solar radiation	8.7
Transmission through clouds	4.9
Clear atmospheric scattering	1.8
Atmospheric radiation	32.3
	<u>47.7</u>

HEAT LEAVING SURFACE VIA

Surface emission	38.5
Evaporation (latent heat transfer)	7.3
Eddy currents (turbulence)	1.0
	<u>47.7</u>

ATMOSPHERIC BALANCE

HEAT ABSORBED BY AIR VIA

Solar radiation	
a. troposphere	5.2
b. stratosphere	1.0
c. clouds	1.2
Surface emission	35.7
Evaporation	7.8
Eddy currents	1.0
	<u>51.9</u>

ATMOSPHERIC RADIATION TO

Space	
a. troposphere	18.6
b. stratosphere	1.0
Earth's surface	32.3
	<u>51.9</u>

NOTE: Numbers shown are average values in  $\text{mw/cm}^2$  assuming a mean cloud cover of 51% and a surface albedo of .90.

where  $q_{\lambda 0}$  is the zenith atmospheric transmissivity at wavelength  $\lambda$ .  $S_{\lambda}$  is the mean solar spectral irradiation at  $\lambda$  just outside the atmosphere. The solar constant is related to  $S_{\lambda}$  by

$$S = \int_0^{\infty} S_{\lambda} d\lambda. \quad (3)$$

For solar zenith angles greater than 0 the direct spectral irradiation at the surface is closely approximated by

$$H_{\lambda}(\theta) d\lambda = \frac{r^2}{r_0^2} S_{\lambda} q_{\lambda} \cos\theta d\lambda, \quad (4)$$

where  $q_{\lambda}$  is the monochromatic transmission through the atmosphere at zenith angle  $\theta$  and is related to  $q_{\lambda 0}$  by

$$q_{\lambda} = q_{\lambda 0}^m, \quad (5)$$

where  $m$  is the optical air mass. If  $\theta$  is not close to  $90^\circ$  and the portion of the earth's surface is at sea level, then

$$m = \sec\theta. \quad (6)$$

The value of  $m$  given by Eq. (6) is called the uncorrected air mass. When  $\theta$  is greater than about  $75^\circ$  a corrected air mass figure, given in Appendix I, should be used. Except where otherwise mentioned, we shall assume that  $\theta$  is small enough so that Eq. (6) may be used with little error. If the surface is not at sea level then

$$m = m_0 \sec\theta, \quad (7)$$

where  $m_0$  is the optical air mass for the zenith path from the surface to space.

The total direct solar irradiation for zenith angle  $\theta$  can be found by integrating  $H_{\lambda}(\theta)$  over all wavelengths:

$$H(\theta) = \frac{r^2}{r_0^2} \cos\theta \int_0^{\infty} S_{\lambda} q_{\lambda} d\lambda. \quad (8)$$

Integration of  $H(\theta)$  with respect to time over the course of a day gives the daily direct beam insolation  $Q_D$ ;

$$Q_D = \int_{\text{SUNRISE}}^{\text{SUNSET}} H(\theta) dt \quad (9)$$

Contour curves of  $Q_D$  as a function of latitude and time of year for  $r = 0.7$  can be found in reference 3. Owing to the fact that  $r$  is larger during the north summer than during the south summer, the Southern Hemisphere receives almost 7% more solar radiation on December 22 than the Northern Hemisphere receives on June 22. In the absence of an atmosphere the North Pole would receive the maximum daily insolation during June and July; however, because of the atmosphere, it actually receives the minimum in the Northern Hemisphere. The maximum daily insolation during these months occurs between  $30^\circ$  and  $40^\circ$  north latitude.

## 2. Atmospheric Depletion of Solar Radiation

The selective nature of atmospheric absorption of solar radiation can be seen in Fig. 1. The solar radiation curve for  $\theta = 60^\circ$  is based on values given in Ref. 4. Atmospheric absorption below 0.3 microns is due to ozone, oxygen, and nitrogen. The ozone region (ozonosphere) is distributed mainly between altitudes of 10 and 40 km, the strongest ozone concentration varying, in the middle latitudes, between a low of about 13 km in late winter to a high of about 30 km in late summer.<sup>5</sup> The amount of ozone in a vertical column varies between about 0.2 atm-cm\* to 0.4 atm-cm. On the average, slightly less than three percent of the incoming solar radiation is absorbed in the ozonosphere.

Since there are no strong absorption bands in the visible region of the spectrum, attenuation of solar radiation in this region is due almost entirely to scattering or reflection from clouds. More than half of this scattered radiation reaches the surface in the form of sky light. Because atmospheric scattering of solar radiation is greater for the shorter wavelengths, more of the blue end of the spectrum is scattered out of the incident sunlight than the red end, giving the sky its characteristic color.

The greatest amount of absorbed solar energy lies in the infrared region. The identities of some of the more intense atmospheric infrared absorption bands of importance for our discussion are listed in Table 2. Beyond the carbon dioxide band centered at 15 microns the atmosphere is practically opaque to infrared radiation because of water vapor absorption. Between 16 and 23 microns there exists a "dirty window" filled

\*The number of atm-cm is the length in centimeters of a column of gas at NTP.

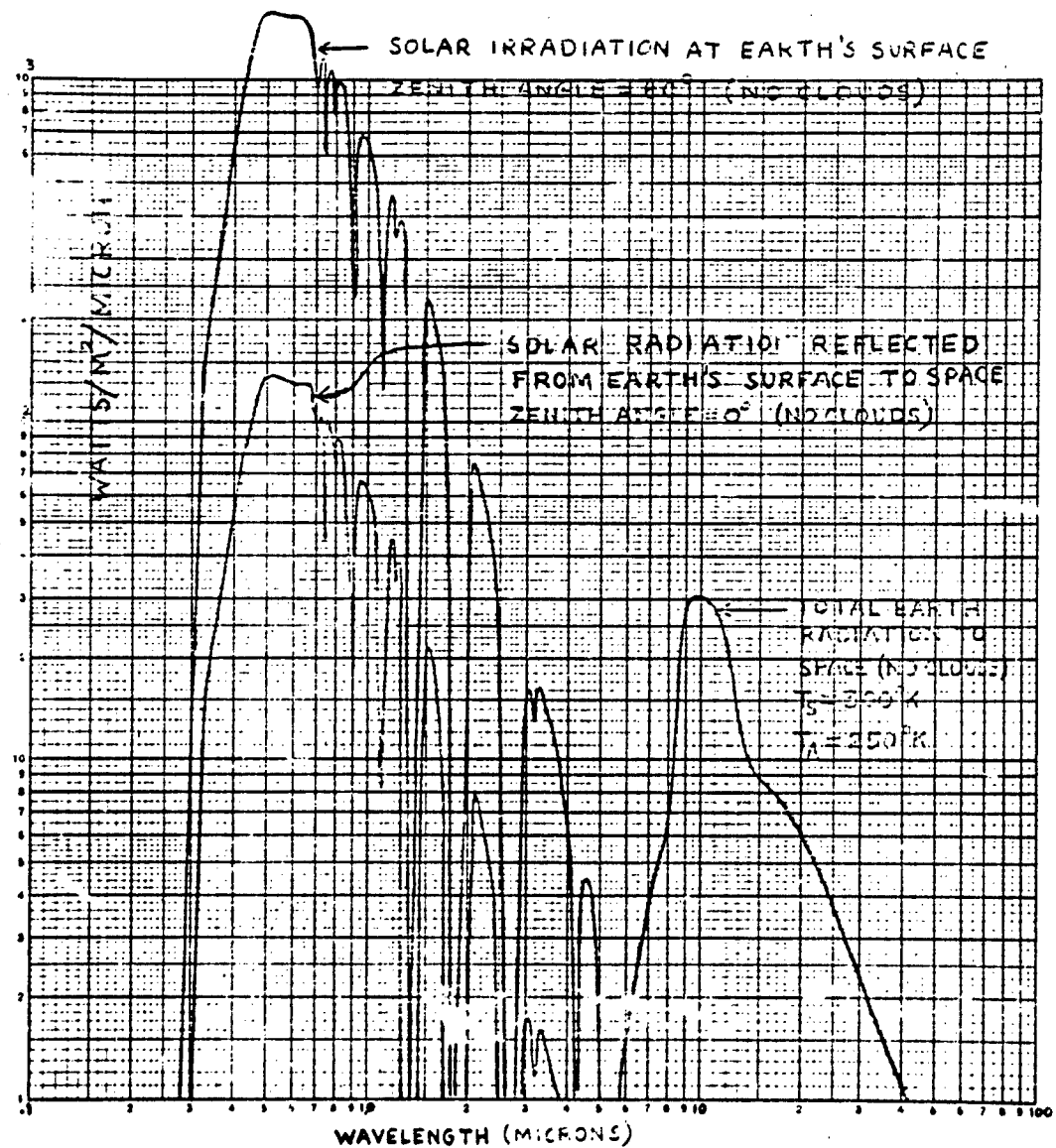


Fig.1. Solar and terrestrial radiation. Reflected solar and total earth radiation to space values should be divided by  $\pi$  to obtain the radiance for each case.  $T_s$  is the surface temperature and  $T_A$  is the effective radiating air temperature.

TABLE 2  
INFRARED ATMOSPHERIC ABSORPTION BANDS

Absorption Wavelength Peak (microns)	Identity of Absorber	Relative Intensity
.72	H <sub>2</sub> O	medium
.76	O <sub>2</sub>	strong
.94	H <sub>2</sub> O	strong
1.13	H <sub>2</sub> O	strong
1.32	H <sub>2</sub> O	strong
1.37	H <sub>2</sub> O	strong
2.01	CO <sub>2</sub>	medium
2.05	CO <sub>2</sub>	medium
2.66, 2.74	H <sub>2</sub> O	strong
2.69, 2.77	CO <sub>2</sub>	medium
3.17	H <sub>2</sub> O	medium
4.26	CO <sub>2</sub>	strong
6.3	H <sub>2</sub> O	strong
9.6	O <sub>3</sub>	strong
15	CO <sub>2</sub>	strong

with many water vapor absorption lines. Transmission data in this region are included in a report by Yates and Taylor<sup>2</sup> who made measurements in the infrared region between the visible and 25 microns. From the data shown in the report it appears that transmission in the 16 to 23 micron region can be ignored when dealing with precipitable water paths greater than about 1 m. Because of the sun's spectral distribution, the amount of solar energy absorbed by the atmosphere in the spectral region beyond 5 microns is relatively small. This is not true for atmospheric absorption of earth surface radiation.

Dust, smoke, and salt particles also absorb (and scatter) solar radiation. The amount of absorption is variable but usually not very great except when the sun is near the horizon. Houghton<sup>1</sup> accounts for depletion of solar radiation by dust, smoke, and salt particles by assuming a dust transmission of  $(0.95)^m$ , where  $m$  is the optical air mass. This transmission expression includes the effects of both absorption and scattering. Of the total dust depletion of solar radiation London<sup>3</sup> assumes that 1/4 is absorbed, 1/4 is scattered back, and 1/2 is scattered forward. A large portion of solar radiation scattered by an unclouded atmosphere is caused by Rayleigh scattering, which is highly wavelength dependent (the scattering

coefficient is inversely proportional to the fourth power of the wavelength). This phenomenon exists when the aerosol particle size is much smaller than the radiation wavelength. Particle diameters less than  $1/10$  wavelength are sufficient to allow use of Rayleigh's scattering formula, according to which the intensity of the scattered radiation is proportional to  $(1 + \cos^2 A)$ , where  $A$  is the angle between the scattered and incident directions. For Rayleigh scattering, therefore, the total radiation scattered in the forward direction is equal to the total radiation scattered backward. Rayleigh scattering occurs for all small particles (compared to the wavelength) including air molecules. As the particle size approaches the wavelength, the Rayleigh theory breaks down and, among other changes, the scattering becomes more directional in favor of the forward direction. For water droplets (which are about as large or larger than the wavelengths considered here) London<sup>8</sup> assumes three times more scattering forward than backward. We shall assume that of the solar radiation scattered by all constituents of a cloud-free atmosphere about 40% is scattered back to space, on the average.

A schematic summary of atmospheric depletion of solar radiation is shown in Fig. 2. Incident solar radiation averaged over the entire surface of the earth is taken as 100 units (equivalent to  $35 \text{ mw/cm}^2$ ). Included in the diagram are absorption and reflection values at the earth's surface. The numbers shown are average values integrated over all angles (during daylight).

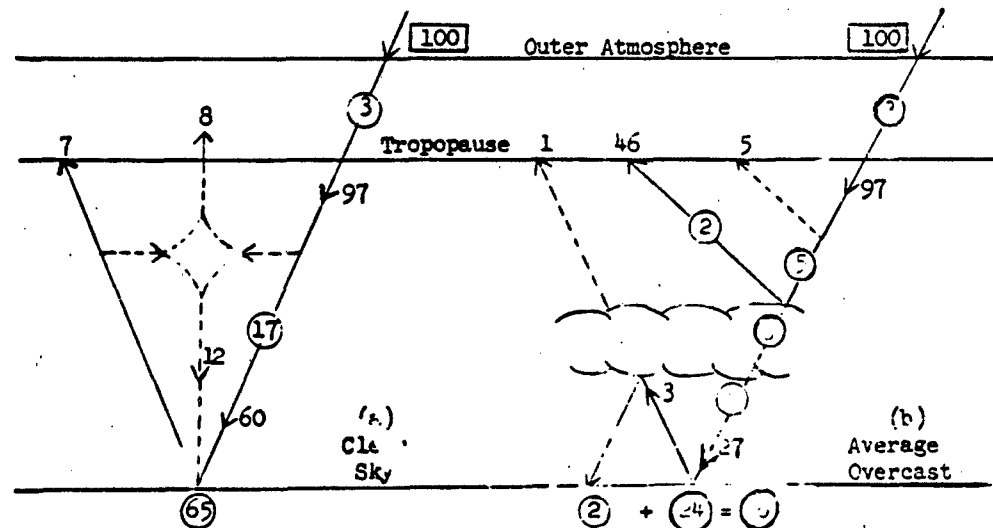


Fig. 2. Depletion of solar radiation. (a) Clear sky condition. (b) Average overcast condition, assuming a mean cloud albedo of 0.55. Circled numbers indicate absorption; uncircled numbers indicate scattering or reflection. Dashed lines signify scattering. The mean surface albedo is assumed to be .10. To average over all weather conditions multiply tropospheric figures shown in (a) by .40 and in (b) by .54.



## 1. Albedo of the Earth

Albedo is a term used to describe the reflecting power of a heavenly body or portion thereof. Since the reflectivity of a material is generally wavelength dependent it is not unusual to find differing albedo values in the ultraviolet, visual, and infrared regions of the spectrum. The total albedo is defined as the ratio of the total power (over all wavelengths) reflected to the total incident power. Since the reflectivity of a surface also depends upon the angle of incidence, the albedo of a flat surface will not be the same as that of a sphere made of the same material.

Therefore, the term spherical albedo is used when referring to a planet as a whole to distinguish it from the reflecting power or albedo of a portion of the planet. Since the satellite radiometer we have in mind views a relatively small portion of the earth at any instant, it is important to understand this difference. Unless otherwise specified the albedo of a surface (grass, sand, etc.) means the total plane albedo at normal incidence. A list of albedos of various terrestrial features is given in Table 3. The spherical albedo values are based on the simplifying assumption that water and clouds are (on a large scale) evenly distributed about the earth. Since atmospheric scattering increases with increasing wavelength it is not surprising to find that the ultraviolet spherical albedo is the largest and the infrared the smallest of the three spectral albedos shown in Table 3(a). In addition, selective absorption by the surface and atmosphere further reduces the value of the infrared albedo.

TABLE 3  
ALBEDOS OF VARIOUS EARTH FEATURES

MATERIAL	ALBEDO	MATERIAL	ALBEDO
Grass	.14 - .37	Forest, Green	.03 - .10
Earth, Dry	.08 - .14	Sea Water, Average	.09 S
Earth, Wet	.08 - .09	Whole Surface, Av.	.10 S
(a) Sand (Desert)	.24 - .28	Whole Earth, UV	.50 S
Snow, Fresh	.80 - .90	Whole Earth, Visible	.40 S
Snow, Old	.45 - .70	Whole Earth, IR	.28 S
Rock	.12 - .15	Whole Earth, Total	.35 S
(b) Solar Zenith Angle (Deg)	0	40	50
Albedo	.03	.03	.04
		.06	.12
			.25
			.40

(a) Albedos of common types of land surfaces, sea water, and the earth as a whole, including the atmosphere.<sup>9-12</sup> The letter S after the numerical value indicates spherical albedo. (b) Albedo of sea water as a function of the solar zenith angle.<sup>13</sup>

Albedo measurements of small sections of the earth taken with the radiometer will vary noticeably as the satellite orbits the earth. In addition to the variable surface albedo there is a very wide range of cloud albedos, depending on drop size distribution and liquid water content. The variation in albedo for different cloud types is shown in Table 4. Although an albedo of 0.85 was observed in a few instances it seems to be the exception rather than the rule. The average albedo for stratus clouds more than 1,000 feet thick was found to be slightly less than 0.70. Averaging over all clouds Fritz<sup>12</sup> estimates the mean cloud albedo to be 0.55. Weiburger<sup>13</sup> found a mean stratus cloud absorptivity of about 0.97. This gives a mean cloud diffuse transmissivity of approximately 38%. Fluctuations from this mean can be great. For a particularly large, dense cloud it is possible to have a diffuse transmissivity of only a few percent.

TABLE 4  
CLOUD ALBEDOS

SOURCE	CLOUD TYPE	ALBEDO
(a)	Luckiest	.75
	(visible light)	Dense clouds, quite opaque .55 - .62
		Dense clouds, nearly opaque .44
		Thin clouds .3 - .40
Fritz (total radiation, extensive systems)	Stratocumulus, overcast	.50 - .81
	Altostratus, occasional breaks	.17 - .36
	Altostratus, overcast	.33 - .59
	Cirrostratus and altostratus	.40 - .64
	Cirrostratus, overcast	.44 - .50
STRATUS CLOUD THICKNESS (FEET)		RANGE OF ALBEDOS
(b)	Greater than 1,000	.60 - .85
	500 - 1,000	.40 - .70
	Less than 500	.10 - .50

- (a) Average albedos of various cloud types.<sup>12</sup>  
 (b) Variation in albedo for stratus clouds of different thicknesses.<sup>13</sup>

#### Terrestrial Radiation

##### 1. Variation with Latitude

Simpson's<sup>15,16</sup> computations for the terrestrial radiation to space at various latitudes is shown in Fig. 3. At the time Simpson made his calculations, little accurate information existed on the absorption spectrum of water vapor; however, the curves of Fig. 3 are probably not very far from the truth. The curve for clear sky condition decreases with increasing

latitude as expected, since surface temperature, on the average, decreases with increasing latitude. For overcast conditions, essentially no surface radiation goes directly to space because it is absorbed by the atmosphere. Under these conditions most of the radiation to space comes from a level somewhat below the tropopause (tropopause temperature increases with increasing latitude). In the polar regions it was assumed that clouds make little difference since they have approximately the same temperature and emissivity as the earth's surface.

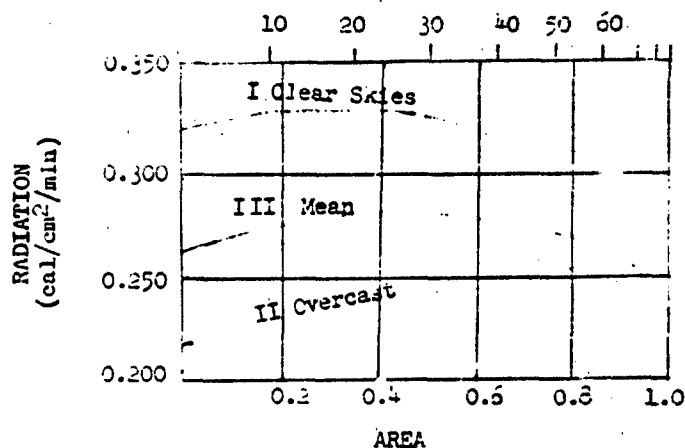


Fig. 3. Terrestrial radiation to space as a function of latitude. The latitude scale is chosen so as to give equal weight to areal belts about each line of latitude.<sup>10</sup>

## 2. Surface Radiation and Atmospheric Absorption

As can be seen from Table 5, all sizeable portions of the earth's surface radiate like blackbodies. Surface temperatures vary from a low of about 220°K to a high of about 320°K. The temperature of the stratosphere varies from about 190°K over the equator to 220°K over the poles. Except for the 8-13 micron window, the atmosphere is essentially opaque to surface radiation. Within this window there is a small amount of ozone absorption centered at 9.6 microns. For complete overcast conditions even the 8-13 micron window is closed to surface radiation.

The 8-13 micron window is bounded by water vapor absorption on the short wavelength end and carbon dioxide on the long wavelength side. Carbon dioxide is fairly uniformly distributed in the atmosphere (.03% by volume), decreasing slightly with altitude. This uniformity does not hold for water vapor, which over North America varies in vertical depth from a low of 1 or 2 mm of precipitable water during winter to a high of 60 or 70 pr. mm during the summer.<sup>10</sup> Since the water vapor absorption bands inside the 8-13 micron

window are fairly weak, the decrease in transmission within this window due to absorption is not a fast-moving function of the precipitable water path. However, high humidity is ideal for formation of water droplets which appreciably increase the scattering of infrared radiation.

TABLE 5  
EMISSIONS OF VARIOUS TERRESTRIAL FEATURES

MATERIAL	EMISSION
Grass	.96
Earth, Dry	.90 - .95
Earth, Wet	.98
Desert	.89 - .91
Snow	.995
Water	.92 - .93
Whole Surface, Average	.93

NOTE: The temperature of the surface is assumed to be between 220 and 320°K.

If the earth's surface is assumed to have a mean surface temperature of 293°K and an emissivity of .93, then the radiation which leaves the ground is 38.9 mw/cm<sup>2</sup>. This figure is found simply by use of the Stefan-Boltzmann law, which is

$$W = \epsilon \sigma T^4, \quad (10)$$

where

W = Radiant emittance (power per unit area)

$\epsilon$  = emissivity

T = absolute temperature

$\sigma$  = Stefan-Boltzmann constant =  $5.672 \times 10^{-8}$  W/M<sup>2</sup>/deg<sup>4</sup>.

However, the atmosphere even under cloudless sky conditions permits only about 18% of this radiation to reach space (see Appendix 2). Therefore, about 7.0 mw/cm<sup>2</sup> reaches space when no clouds are present. For a mean cloud cover of 54% the average surface emission that penetrates the atmosphere is only 3.2 mw/cm<sup>2</sup>. The remaining 35.7 mw/cm<sup>2</sup> which comes from the earth's surface is absorbed by the atmosphere, on the average.

### 3. Self-Emission by the Atmosphere

Water vapor is the major source of long-wave radiation to space. In the lower atmosphere it radiates with relatively high emissivity and a

fairly warm average temperature, but most of the outward bound radiation is absorbed and reradiated by progressively rarer and cooler water vapor. Above the tropopause, emission by water vapor is small. The apparent water vapor radiance as measured by a satellite radiometer should be the same as that of a blackbody at a temperature which is equal to the upper troposphere temperature.

If we take .35 as the mean total planetary albedo, then 65% of solar radiation is absorbed by the earth's surface and atmosphere, on the average. Since the global mean temperature has changed very little over the last century, it is safe to assume that all the solar energy absorbed is radiated back to space (but in a different wavelength region). Therefore, the average outgoing planetary radiant emittance is (.65) (S/4) or 22.8 mw/cm<sup>2</sup>, which is equal to the total radiant emittance of a blackbody at 252°K (equivalent blackbody temperature). It should be pointed out that the concept of equivalent blackbody temperature should be used with caution, especially if the body in question has a low emissivity or is a selective emitter. For example, it is not safe to hold (with bare hands) a polished aluminum sheet (emissivity = 0.1) that is radiating with an equivalent blackbody temperature of 290°K (17°C or 62°F), because the actual temperature of the aluminum is 515°K (432°F).

As mentioned earlier the stratosphere absorbs slightly less than 3% of solar irradiation. If the stratosphere is in over-all radiative equilibrium, it must have a mean radiant emittance of (.03) (S/4) or 1.0 mw/cm<sup>2</sup>. This radiation is due to carbon dioxide and water vapor with a small contribution by ozone. The mean long-wave radiation to space is divided up as follows: mean surface radiation - 3.2 mw/cm<sup>2</sup>, stratosphere - 1.0 mw/cm<sup>2</sup>, troposphere - 13.6 mw/cm<sup>2</sup>.

#### Radiation in Five Spectral Regions

##### 1. Region One: 0.2 - 5.5 Microns

In this region the outgoing energy is due to reflected and scattered solar radiation. The contribution from the portion of the earth's surface (assumed to be a diffuse reflector) within the detector's field of view is

$$N_A = \rho \frac{S}{\pi} \cos \theta \cos \phi q_\theta q_\phi, \quad (11)$$

where

- $N_A$  = apparent surface radiance (power/area/solid angle)
- $\rho$  = surface reflectivity
- $S$  = solar constant = 140 mw/cm<sup>2</sup>
- $q_\theta$  = mean atmospheric transmission of incident solar radiation for sun at zenith angle  $\theta$
- $q_\phi$  = mean atmospheric transmission of reflected solar radiation for detector zenith angle  $\phi$ .

Zenith angles  $\theta$  and  $\phi$  are measured from the portion of the surface within the detector's instantaneous field of view. It should be pointed out that the look angle of the detector (i. e., the angle measured from the vertically downward direction at the detector to the portion of the surface within the detector's field of view) is approximately equal to  $\phi$  for small zenith angles only. The relationship between detector look angle and  $\phi$  is discussed in Appendix 3.

If the instantaneous atmospheric absorption and scattering coefficients are not single-valued functions of altitude over a broad area, then the transmissions  $q_\theta$  and  $q_\phi$  are dependent on azimuthal angles as well as zenith angles. Even if the transmissions were not dependent on azimuthal angles,  $q_\theta$  would not precisely equal  $q_\phi$  when  $\theta = \phi$ , because the average transmission over a spectral region containing many atmospheric absorption lines does not follow the simple exponential absorption law for a single isolated absorption line. However, for the sake of simplicity, we shall assume that the mean transmission at any zenith angle  $\psi$  can be expressed with a fair degree of accuracy by

$$q_\psi = q_0^m, \quad (12)$$

where

$q_0$  = mean transmission at  $\psi = 0$

$m$  = optical air mass at angle  $\psi$ .

For  $\psi$  less than about  $70^\circ$  or  $75^\circ$  we can express  $m$  in the same form given in Eq. (7),

$$m = m_0 \sec \psi, \quad (13)$$

where  $m_0$  is the mean optical air mass for  $\psi = 0$ . For a path between space and sea level  $m_0 = 1$ . For air masses at angles greater than about  $75^\circ$  see Appendix 1.

From Eq. (11) we see that the maximum values of  $N_A$  occur at  $\phi = 0$  in those regions (and times) where  $\rho$  is high,  $\theta_{\min}^*$  and  $m_0$  are small. However, except for certain snow-capped mountains, snow does not normally occur at the lower latitudes when  $\theta_{\min}$  is small. Also, the value of  $q_0$  near sea level is generally higher in regions where  $\theta_{\min}$  is small. For a snow-capped mountain we shall assume that  $\rho = .85$ ,  $\theta_{\min} = 0$ ,  $\phi = 0$ , and  $q_\theta = q_\phi = .85$  to obtain a reasonable maximum value of  $N_A$  for the earth's surface. Therefore,

\* $\theta_{\min}$  is the minimum solar zenith angle reached during the course of the day.

$$N_A (\text{max}) = (.85) \frac{140}{\pi} (.85)^2$$

$$= 27 \text{ mw/cm}^2/\text{ster (snow capped mountain).}$$

For snow at sea level we shall assume that  $\rho = .85$ ,  $\theta_{\min} = 35^\circ$ ,  $\phi = 0$ , and  $c_0 = .75$ . Therefore,

$$N_A = (.85) \frac{140}{\pi} (.819) (.75)^{2.22}$$

$$= 16 \text{ mw/cm}^2/\text{ster (snow at sea level).}$$

The lower-lying thick clouds generally have high albedos. Very thick stratus clouds have albedos in the neighborhood of .75 although albedos as high as .85 have been recorded in a few instances. Atmospheric transmission of reflected solar radiation from stratus clouds to space is about .85 (for  $\phi = 0$ ). Therefore,  $N_A$  for very thick stratus clouds is almost as high as that for the snow-capped mountain. Since the average stratus cloud has an albedo of about .55, which is much higher than that of most of the earth's surface, the majority of high level signals received in region one (0.2 - 5.5 microns) will come from clouds. Table 6 shows apparent radiance values for various types of surfaces and different cloud thicknesses due to reflected solar radiation.

TABLE 6  
APPARENT RADIANCE VALUES OF VARIOUS EARTH SURFACE FEATURES

FEATURE	REFLECTIVITY	APPARENT RADIANCE (mw/cm <sup>2</sup> /ster)
Snow-capped mountain	.85	27
Snow at sea level	.85	16
Desert	.25	6.3
Earth	.10	2.5
Rock	.14	3.5
Forest	.06	1.5
Water	.03	0.8
Very thick stratus clouds	.75	24
Average stratus clouds	.55	18
Thin stratus clouds	.38	13

Apparent radiance values of various earth surface features in region one (0.2 - 5.5 microns) due to reflected solar radiation. Solar and detector zenith angles are assumed to be 0 except for the snow at sea level feature where the solar zenith angle is taken as  $35^\circ$ .

## 2. Region Two: 8 - 30 Microns

In this region the radiation received by the detector will be due almost entirely to the self-emission by the earth's surface and atmosphere. The radiation received from any portion of the earth's surface is confined to the 8 - 13 micron window. Assuming the earth's surface to radiate as a graybody with an emissivity of .93 then the apparent radiance in the 8 - 13 micron region under clear sky conditions is given by

$$N_A = .93 C_1 \int_8^{13} \frac{q_{o\lambda}^m d\lambda}{\lambda^5 \left[ \frac{C_2}{\lambda T} - 1 \right]} \quad (14)$$

where

$C_1$  = 11.9 for  $N_A$  in  $\text{mw}/\text{cm}^2/\text{ster}$

$C_2$  = 14,400 micron-degrees K

$\lambda$  = wavelength in microns

$T$  = temperature in K

$q_{o\lambda}$  = atmospheric transmission at wavelength  $\lambda$  for 0 zenith angles

$m$  = optical air mass ( $m$  is a function of zenith angle  $e$ ).

Equation (14) is too complex to be treated analytically. However, it can be approximated without large error by

$$N_A = .93 q_o^m C_1 \int_8^{13} \frac{d\lambda}{\lambda^5 \left[ \frac{C_2}{\lambda T} - 1 \right]} \quad (15)$$

where  $q_o$  is the mean transmission in the 8 - 13 micron region for 0 zenith angle. Figures 4 and 5 show the apparent radiance values in the 8 - 13 micron region as a function of detector zenith angle for various earth surfaces when  $q_o$  is .75 and .85, respectively.

The apparent self-radiance of the atmosphere is primarily due to water vapor (and droplets). Since water vapor emissivity is a function of the amount of precipitable water in the path, the apparent radiance of the atmosphere will vary with detector zenith angle  $e$ . However,  $N_A$  will not vary rapidly with  $e$ . For a water path of only 2 or 3 pr. mm the average emissivity in this region (8 - 30 microns) at a temperature of 250°K is already appreciable (about .3). Thick dense clouds have an emissivity of



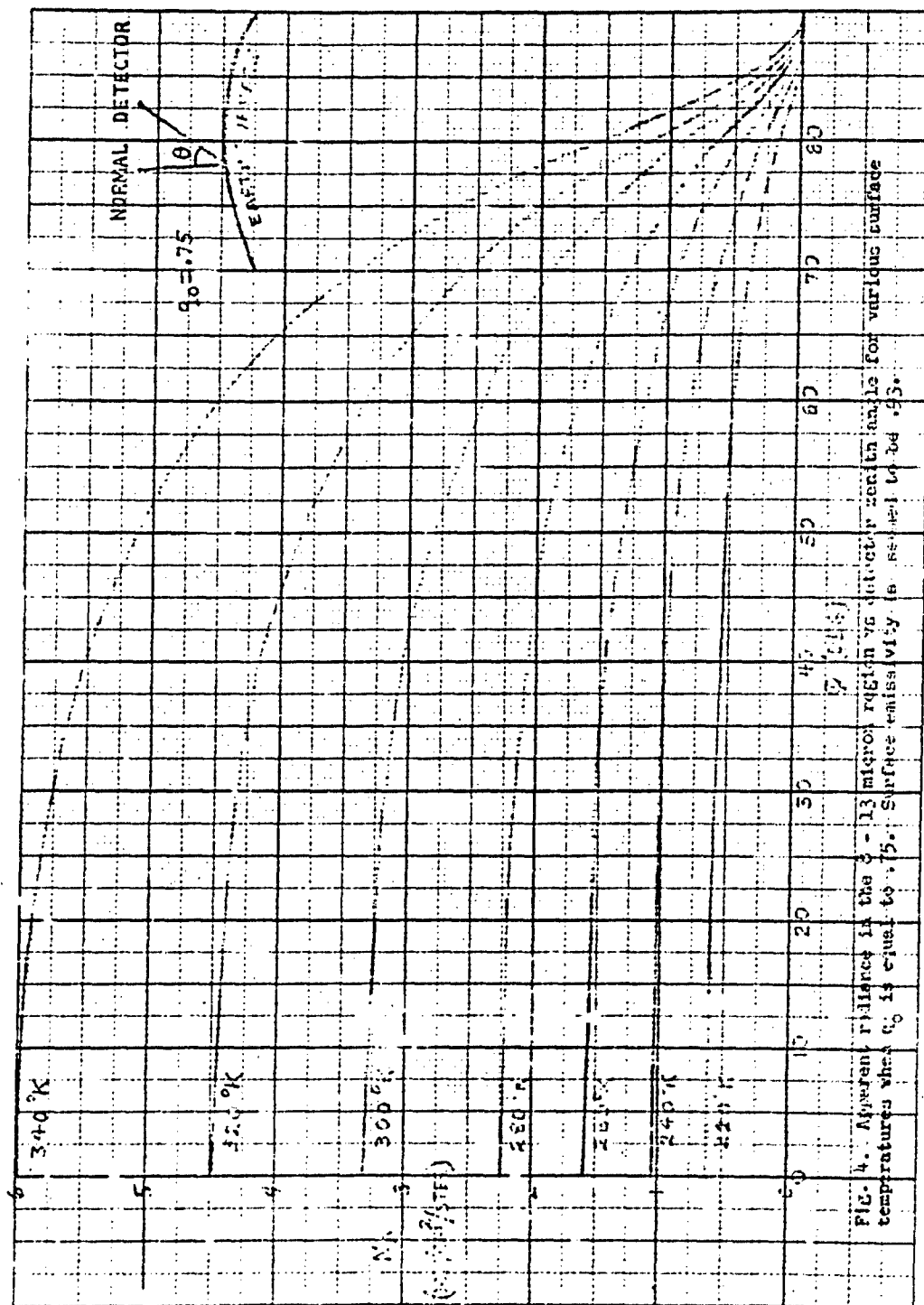


FIG. 4. Apparent radiance in the 3-13 micron region vs. detector zenith angle for various surface temperatures when  $q_0$  is equal to 75. Surface emissivity is assumed to be .95.

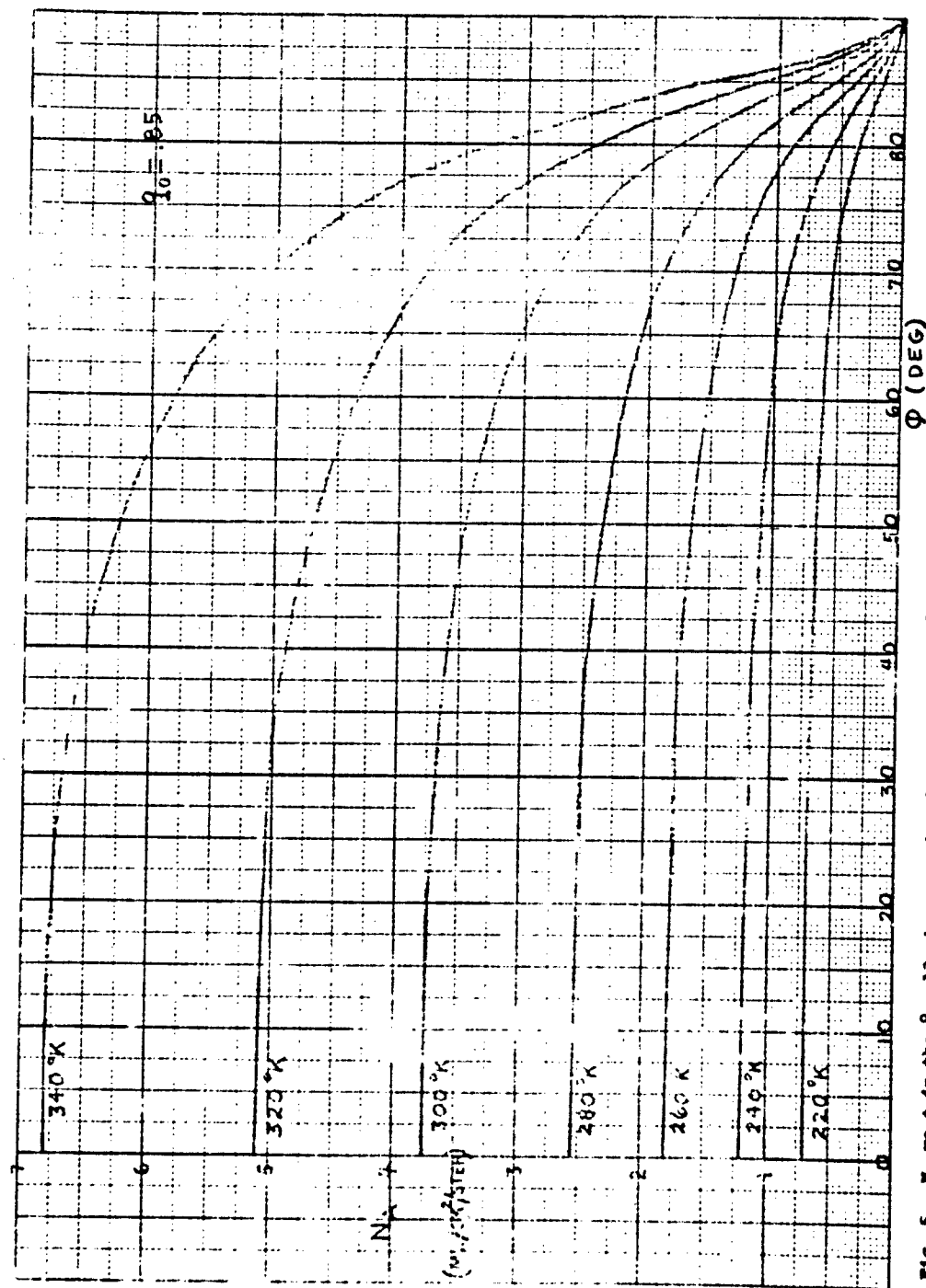


Fig. 5.  $N_A$  vs  $\phi$  in the 8 - 13 micron region for  $q_0$  equal to .85.

about 1 and, therefore, have an apparent radiance equal to that of a portion of the earth's surface which is at the same temperature as the cloud top. Since clouds are usually cooler than the ground below, it can be expected that clouds will often have a lower apparent radiance than the adjacent ground areas. However, the reverse is true for those conditions when clouds are warmer than the ground. In general, the difference in radiance between cloud and ground should be small, although in extreme cases the ground can have twice the radiance of a dense cloud.

In order to obtain a maximum unclouded atmospheric radiance value we shall assume that over the warm regions of the earth the atmosphere radiates as a graybody at  $270^{\circ}\text{K}$  with an average zenith emissivity ( $\epsilon = 0$ ) of .5 in the 8 - 12 micron spectral region. With these assumptions we obtain for unclouded conditions at  $\epsilon = 0$

$$N_A = 3.5 \text{ mw/cm}^2/\text{ster (atmosphere)}.$$

If the ground is at a temperature of  $320^{\circ}\text{K}$  and  $q_0 = .75$  we see from Fig. 5 that at  $\epsilon = 0$ , assuming no clouds,

$$N_A = 4.5 \text{ mw/cm}^2/\text{ster (ground)}.$$

For these conditions the detector will measure an apparent radiance of 8 mw/cm<sup>2</sup>/ster. If this region is covered with dense clouds with an average temperature of, say,  $280^{\circ}\text{K}$  then the total radiance for  $q_0 = .35$  will be 8 mw/cm<sup>2</sup>/ster. The lowest radiance values that can be expected will occur in regions where the ground temperature is approximately  $220^{\circ}\text{K}$  ( $q_0 = .85$ ) and the atmosphere is at about the same temperature with an average zenith emissivity of .3. For this case the total radiance at  $\epsilon = 0$  is about 1.9 mw/cm<sup>2</sup>/ster. If cloud cover is present the total radiance figure will not change appreciably.

### 3. Region Three: 8 - 12 Microns

The 8 - 12 micron bandwidth is intended for the measurement of radiation from the earth's surface and clouds. Since the surface radiation that reaches space in this region is almost the same as that in region two, Figures 4 and 5 may be used for radiation estimates. For greater accuracy the values shown in the figures should be reduced by 10% for region three.

The difference in the received radiation between that of channels two and three will be a measure of the contribution to the space radiation by the unclouded atmosphere. The radiation received by the unclouded atmosphere in channel three will be much lower than that for channel two (8 - 30 microns). In addition to the smaller bandwidth of channel three the average zenith emissivity of the atmosphere in region three is about 1/3 that for region two. The mean zenith atmospheric radiance for an average air temperature of  $270^{\circ}\text{K}$  is only 0.35 mw/cm<sup>2</sup>/ster for region three, which is

1/10 that for the 8 - 30 micron region. The corresponding maximum radiance in this channel under the same assumptions made for channel two (ground temperature of 320°K,  $q_0$  of .75, no clouds) is 4.4 mw/cm<sup>2</sup>/ster.

#### 4. Region Four: 0.55 - 0.75 Microns

The visible region is well suited for determining cloud cover under daylight conditions since the contrast between clouds and most surface features is generally high. The red end of the visible spectrum (.55 - .75 microns) is a particularly good region because there is less scattering of solar radiation by the atmosphere in this region than in the blue end of the spectrum (this is the reason that the sky appears blue). A little over 19% of all solar radiation is concentrated in region four. Since the solar constant is 140 mw/cm<sup>2</sup>, about 27 mw/cm<sup>2</sup> enters the earth's atmosphere (at normal incidence) in this spectral region. For radiance calculations we may use Eq. (11) if we replace the solar constant S in that equation by .193. Therefore, for region four

$$N_A = 8.6 \rho q_0 q_\phi \cos\theta \cos\phi, \quad (16)$$

where the symbols used have the same meaning as before. Clouds have a large range of reflectivity depending on cloud type and thickness. For thick, dense clouds with a reflectivity of .75 the apparent radiance is, assuming  $\theta = \phi = 0$ ,  $q_\phi = .93$ :

$$N_A = (8.6) (.75) (.93)^2 = 5.6 \text{ mw/cm}^2/\text{ster}.$$

The reflectivity of surface features in region four is approximately the same as the albedo figures shown in Table 3. The lowest reflectivity that can be expected for the darkest surface is about .030. For  $q_\phi = .90$  this yields an apparent zenith radiance of

$$N_A = (8.6) (.030) (.90)^2 = 0.21 \text{ mw/cm}^2/\text{ster}.$$

Actually this figure will be higher because of the radiation scattered back by the atmosphere. If we take .015 as a reasonable value for zenith "air reflectivity" then the above radiance value becomes 0.33 mw/cm<sup>2</sup>/ster. For  $\theta = \phi = 0$ , atmospheric scattering between cloud top heights and space does not contribute significantly to the value of  $N_A$  for clouds. For clouds, therefore, the maximum to minimum radiance ratio that can be expected in region four is 17. This ratio will become smaller if  $\theta$  and  $\phi$  increase.

For channel four when the detector is looking at snow-covered regions the apparent radiance will be somewhat higher than that of thick dense clouds and almost 50% higher than average stratus clouds. For  $q_\phi = .90$  the apparent snow radiance is 5.9 mw/cm<sup>2</sup>/ster. If the contribution of atmospheric scattering is included,  $N_A$  for snow is 6.0 mw/cm<sup>2</sup>/ster.

#### 1. Region Five: 5.7 - 6.3 Microns

This region covers one of the most intensive water vapor absorption bands in the electromagnetic spectrum. Practically speaking, no radiation other than that due to water vapor emission leaves the atmosphere in this region. Because of the great absorptivity, emission by water vapor in this band, in the lower atmosphere, is absorbed and reradiated (at a lower temperature) by water vapor in the higher layers of the atmosphere. Above the tropopause there is so little water vapor that even 6.3-micron radiation goes through without a great deal of attenuation. Effectively, this radiation will appear to come from an altitude somewhat below the tropopause.

Received radiation will therefore be a measure of the tropopause temperature.

Since the tropopause temperature varies from about 190°K over the equator to 240°K over the poles, the apparent radiance in the wavelength region between 5.7 and 6.3 microns should vary from about .01 mW/cm<sup>2</sup>/ster to about .03 mW/cm<sup>2</sup>/ster. Actually, the tropopause region does not contain a sufficient amount of water to completely absorb the 6.3-micron radiation coming from the neighboring region below it. Although the water vapor concentration increases with decreasing altitude below the tropopause, so does the temperature (except possibly at the poles). The net result is an effective radiation temperature which is higher than the 190 - 220°K range shown. Results from TIPS II-1 indicate an effective radiation temperature range of about 110-155°K, which gives an apparent radiance level range of .01 to .10 mW/cm<sup>2</sup>/ster in region five.

#### 1.1 Calculations

If the received radiation comes from an area which completely fills the detector's instantaneous field of view (assumed to be small), then the flux received by the detector,  $P$ , in a specified spectral region,  $\Delta\lambda$ , can be given by

$$P_{\Delta\lambda} = H_{\Delta\lambda} \cdot \Omega \cdot A_e \cdot t_{\Delta\lambda} \quad (17)$$

where

- $H_{\Delta\lambda}$  = apparent radiance of the target in the spectral region  $\Delta\lambda$
- $\Omega$  = instantaneous solid angle field of view
- $A_e$  = effective aperture area
- $t_{\Delta\lambda}$  = effective transmission of optical system in the spectral region  $\Delta\lambda$ .

The calculated signal-to-noise ratio in the spectral region  $\Delta\lambda$  is

$$(S/N)_{\Delta\lambda} = \frac{P_{\Delta\lambda}}{P_N} = \frac{N_{\Delta\lambda} \Omega A_M t_{\Delta\lambda}}{P_N} \quad (18)$$

where  $P_N$  is the noise equivalent power of the detector. If we let  $V_N$  be the RMS noise voltage at the output of the bolometer bridge, then

$$P_N = \frac{V_N^2}{r} \quad (19)$$

where  $r$  is the bolometer bridge responsivity. For the purpose of illustration we shall calculate signal-to-noise ratios for the satellite radiometer described in Ref. 1 which employs thermistor bolometers as detectors. For our purpose the important radiometer characteristics (taken from Ref. 1) are:

$$\begin{aligned} A_M &= .63 \text{ cm}^2 \\ \Omega &= .009 \text{ steradians} \\ V_N &= .65 \text{ microvolts} \\ r &= 21 \text{ volts/watt} \end{aligned}$$

Channel	1	2	3	4	5
$t_{\Delta\lambda}$	.90	.21	.15	.55	.35

Table 7 lists the maximum value of  $S/N$  that can be expected for each channel. If the system noise and responsivity are different from that assumed above ( $t_{\Delta\lambda}$  assumed to remain constant) then the  $S/N$  values given in Table 7 should be multiplied by

$$3.1 \times 10^{-8} \frac{r}{V_N} = \frac{3.1 \times 10^{-8}}{P_N}$$

where  $r$  is measured in volts/watt,  $V_N$  in volts, and  $P_N$  in watts.

TABLE 7  
MAXIMUM VALUE OF S/N FOR EACH CHANNEL

CHANNEL	BANDWIDTH (Microns)	$N_A$ (Max) (mw/cm <sup>2</sup> /ster)	S/N (Max)
1	.2 - 5.5	27	4,500
2	8 - 30	8.0	300
3	8 - 12	4.4	120
4	.55 - .75	6.3	640
5	5.5 - 6.9	.18	12

The values for channel 1 are for a snow-capped mountain in the lower latitudes. If the detector's field of view is greater than the snow-covered region the S/N will be smaller than that shown.

#### SUMMARY

A study is made of planetary radiation received by a satellite radiometer looking at various portions of the earth's surface and atmosphere. The received radiation is divided into five spectral regions or channels. The wavelengths and purpose of each channel are given below:

- (1) 0.2 - 5.5 microns (total albedos of the earth)
- (2) 8 - 30 microns (total emission from the earth)
- (3) 8 - 12 microns (surface and cloud emission)
- (4) 0.55 - 0.75 microns (cloud cover)
- (5) 6.3 ± 10% microns (tropopause temperature)

In order to intelligently interpret the data received by the satellite radiometer it is essential to understand the contributions made by the sun, earth's surface, and atmosphere in the five spectral regions listed above.

a. Sun: Radiates essentially as a blackbody at 5800°K. Over 99% of the radiation reaching the earth lies in the 0.2 - 5.5 micron spectral region.

b. Earth's Surface: Even at 310°K (98°F) the earth's surface emits less than 3% of its radiation in the channel one region (0.2 - 5.5 microns). Much less than 3% of the radiation in this spectral region reaches space because of absorption and scattering by the atmosphere. The major portion of surface radiation which reaches space lies in the channel three region (8 - 12 microns).

c. Atmosphere: The atmosphere plays a dominant role in terrestrial radiation because of its scattering, reflecting (clouds), radiating, and selective absorption properties. On the average, assuming a mean cloud cover of 54%, the atmosphere absorbs 17% and reflects or scatters out about 31% of solar radiation. Of the total outgoing planetary radiation due to

self-emission, 86% comes from the atmosphere, the remaining 14% comes directly from the earth's surface, on the average.

The maximum and minimum radiance levels that can be expected within each channel is shown in the table below.


CHANNEL	BANDWIDTH (Microns)	MAX. RADIANCE (mw/cm <sup>2</sup> /ster)	MIN. RADIANCE (mw/cm <sup>2</sup> /ster)
1	.2 - 5.5	27	0
2	8 - 30	8.0	1.6
3	8 - 12	4.4	1.5
4	.55 - .75	6.0	0
5	5.5 - 6.9	.18	.03

The maximum radiance level for channel one is for a snow-capped mountain in the lower latitudes. If the detector's field of view is greater than the snow-covered region, the apparent radiance as measured by the detector will be lower than that shown. The minimum radiance values listed for channels one and four are for night conditions when the received radiation is below the noise equivalent power of the detector.

#### REFERENCES

1. Design Study of Satellite Meteorological Radiometer System, BEC-4208-1, Barnes Eng. Co. (Nov. 14, 1958).
2. Johnson, F. S., J. Meteorol., vol 11 (1954).
3. Haltiner and Martin, Dynamical and Physical Meteorology, Mc Graw Hill and Co. (1957), p. 96.
4. Smithsonian Physical Tables, 9th Ed. (1954), p. 720.
5. Epstein, Osterberg, and Adel, Scientific Report RA-7, Contract Nr. AF 19(122)-198 (Dec. 1955).
6. Yates and Taylor, Infrared Transmission of the Atmosphere, NRL Report 5453 (June 8, 1960).
7. Houghton, H. G., J. Meteorol., vol 5 (1951).
8. London, J., A Study of the Atmospheric Heat Balance, N. Y. U. Final Report AF 19(122)-165 (July 1957).
9. Fritz, S., J. Meteorol., vol 6 (1949), pp. 277-282.
10. Neiburger, M., J. Meteorol., vol. 6 (1949), pp. 98-104.
11. Falckenburg, G., Met. Z., 45(1928), pp. 334, 422.



- 
12. Brewer and Houghton, Proc. Roy. Soc. A, vol 235 (1956).
  13. Sverdrup, H. U., The Earth as a Planet, vol II (1954), p. 222.
  14. Fritz, S., Compendium of Meteorology (1951), pp. 13-33.
  15. Simpson, G. C., Mem. R. Met. Soc. 3 (1923).
  16. Byers, H. R., The Earth as a Planet, vol. II (1954), pp. 299-370.
  17. Hansel, R., NASA, Goddard Space Flight Center, Greenbelt, Md., private communication.

## APPENDIX 1

### OPTICAL AIR MASS

Although the term "optical air mass" originally referred to the visible region, it is now used for the ultraviolet and infrared regions as well. The concept of optical air mass was developed in an attempt to quantitatively account for the decrease in the apparent brightness of heavenly bodies with increase in zenith angle  $\theta$  under unclouded conditions. If  $q_0$  is the zenith atmospheric transmissivity ( $\theta = 0$ ) at a particular monochromatic wavelength  $\lambda$ , and  $q_\theta$  is the transmissivity at zenith angle  $\theta$ , then the optical air mass  $m$  is defined by the equation

$$q_\theta = q_0^m.$$

In practice  $q_0$  and  $q_\theta$  are never measured using monochromatic radiation.\* If narrow enough bandwidths are chosen the values of  $q_0$  and  $q_\theta$  can be closely approximated for monochromatic radiation. However, use of monochromatic values of transmissivity generally make radiation calculations over nonzero bandwidths very difficult. For simplicity  $q_0$  and  $m$  are evaluated for narrow nonzero bandwidths. When atmospheric attenuation is due primarily to scattering, as is the case throughout most of the visible, fairly accurate predictions can be made using a  $\Delta\lambda$  of, say,  $.05\lambda$ .

The uncorrected optical air mass  $m_u$  (measured from sea level) is given by the simple expression

$$m_u = \sec\theta.$$

This formula is based on the following assumptions:

- a. the earth is flat
- b. there is negligible atmospheric refraction
- c. at any instant of time all atmospheric properties affecting transmission vary with altitude only (not with latitude and longitude).
- d. atmospheric transmission obeys Beer's law

$$q = e^{-kcd\theta},$$

\*A monochromatic wave has a wavelength bandwidth of zero. The amount of radiated energy contained within a zero bandwidth from any real source (lasers included) is precisely 0.

where

$k$  = extinction cross section

$c$  = particle concentration

$dr$  = elemental path length.

Table 8 lists two sets of values of optical air mass for several zenith angles based on (1) the simple secant formula and (2) a more complex formula of Bemporad, which considers earth curvature and atmospheric refraction. Note that the divergence between the two is small except for large zenith angles.

TABLE 8  
OPTICAL AIR MASS AS A FUNCTION OF ZENITH ANGLE<sup>5</sup>

ZENITH ANGLE	0°	60°	70°	80°	85°	88°
SECANT FORMULA	1.00	2.000	2.924	5.76	11.47	28.7
BEMPORAD	1.00	1.995	2.904	5.60	10.39	19.8

For both cases shown it is assumed that atmospheric particle concentration varies with altitude only and that there is no overcast.

Under the assumptions stated, use of Bemporad's values of optical air mass shown in Table 8 will give a fairly accurate relationship between  $q_0$  and  $q_\theta$  for narrow bandwidths in the visible region. The accuracy decreases somewhat for the infrared region where the predominant cause of attenuation is generally due to absorption rather than to scattering. Even for  $\Delta\lambda/\lambda = .05$ , absorption of radiation in the infrared does not follow Beer's law as stated above. For moderate absorber concentrations the error involved in predicting  $q_\theta$  will be tolerable in most instances if  $\theta$  is not large. For large values of  $\theta$  the error becomes appreciable.

## APPENDIX 2

### AVERAGE TRANSMISSION THROUGH A PLANETARY ATMOSPHERE

In order to simplify the problem of determining the average transmission of surface radiation (emission) through an atmosphere in the form of a spherical shell, we make the following assumptions:

- scattering is negligible
- the atmospheric absorption coefficient changes with altitude only
- appreciable absorption occurs only at altitudes which are small compared to the sphere's radius.
- the sphere's surface radiates in accordance with Lambert's cosine law
- the optical air mass  $m_\theta$  at zenith angle  $\theta$  is given by  $m_\theta = \sec\theta$ .

The surface radiant intensity  $J_\theta$  in the x direction (see Fig. 6) leaving the atmosphere from an elemental band  $dA$  subtending an angle  $\theta$  at the sphere's center is

$$dJ_\theta = \frac{W_0}{\pi} \cos\theta q_\theta dA, \quad (20)$$

where

$W_0$  = radiant emission of sphere (power/unit area)

$q_\theta$  = atmospheric transmission in the x direction from elemental area  $dA$ .

The total surface radiant intensity to space in the x direction is therefore

$$J = \int_0^{\pi/2} dJ_\theta = \frac{W_0}{\pi} \int_0^{\pi/2} q_\theta \cos\theta dA. \quad (21)$$

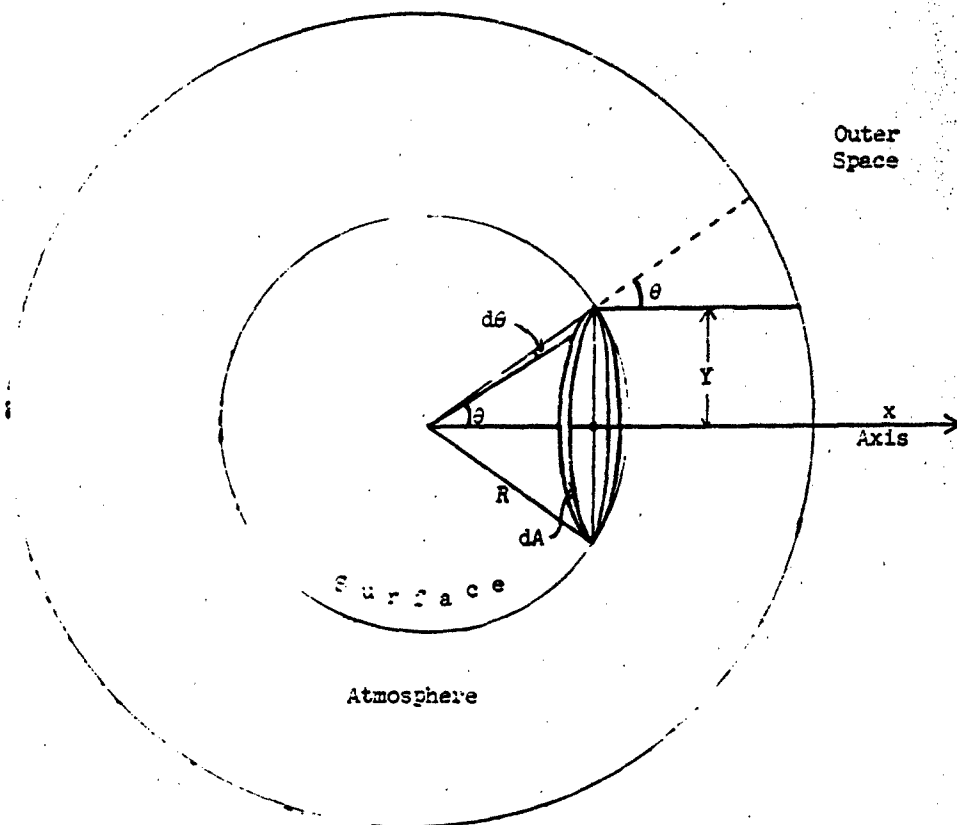


Fig. 6. Geometry for calculating average transmission of a planetary atmosphere. The band  $dA$  is chosen symmetrically about the  $x$  axis.

The average transmission of a planetary atmosphere  $q_{av}$  can be defined as

$$q_{av} = \frac{\int_0^{\pi/2} dJ_{\theta}}{\int_0^{\pi/2} dJ'_{\theta}} \quad (22)$$

where

$$dJ'_{\theta} = \frac{dJ_{\theta}}{q_{\theta}} \quad (23)$$

The denominator in Eq. (22) is the total surface radiant intensity to space, neglecting atmospheric attenuation. From Eqs. (20), (22), and (23) we get

$$q_{av} = \frac{\int_0^{\pi/2} q_s \cos \theta \, dA}{\int_0^{\pi/2} \cos \theta \, dA} \quad (24)$$

The elemental area  $dA$  is equal to the circumference of the band multiplied by the width of the band. Therefore,

$$dA = (2\pi y) (R d\theta). \quad (25)$$

Since  $y = R \sin \theta$  (see Fig. 6),

$$dA = 2\pi R^2 \sin \theta \, d\theta. \quad (26)$$

Substitution of this expression for  $dA$  into Eq. (24) leads to

$$q_{av} = 2 \int_0^{\pi/2} q_s \sin \theta \cos \theta \, d\theta. \quad (27)$$

From assumption (e) we have

$$q_s = q_0^{\sec \theta}, \quad (28)$$

where  $q_0$  is the average value of atmospheric transmission for  $\theta = 0$ . If we let  $u = \sec \theta$ , and

$$q_0 = e^{-k},$$

where  $k$  is a parameter that is independent of  $\theta$ , we get

$$q_{av} = 2 \int_1^{\infty} \frac{e^{-ku}}{u^3} \, du. \quad (29)$$

Integration by parts twice yields

$$q_{av} = e^{-k}(1 - k) + k^2 \int_k^{\infty} \frac{e^{-\alpha}}{\alpha} d\alpha, \quad (30)$$

where  $\alpha = kx$ . The exponential integral in Eq. (30) is tabulated in many tables of integrals. For convenience some values of the integral are shown in Table 9.

TABLE 9  
VALUES OF THE EXPONENTIAL INTEGRAL

$k$	.10	.20	.30	.35	.40	.50	.70	1.0	1.5	2.0
$\int_k^{\infty} \frac{e^{-\alpha}}{\alpha} d\alpha$	1.82	1.22	.906	.794	.702	.560	.374	.219	.100	.049

The average zenith transmission of the earth's atmosphere in the 8 - 13 micron window, assuming no clouds, is about .70 which is equivalent to  $k = .35$ . Therefore,

$$q_{av} (8-13\mu) = (.70) (1 - .35) + (.35)^2 (.794) = .55.$$

A blackbody at 293°K radiates 32% of its energy in the 8 - 13 micron region. Since the atmosphere is effectively opaque to 293°K radiation outside this region, only (.55) (.32) or 18% of surface radiation is transmitted through a cloudless atmosphere, on the average.

# APPENDIX 3

## SATELLITE DETECTOR LOOK ANGLE AND ZENITH ANGLE

Figure 7 illustrates the relationship between detector look angle and zenith angle. Atmospheric refraction is ignored in this discussion.

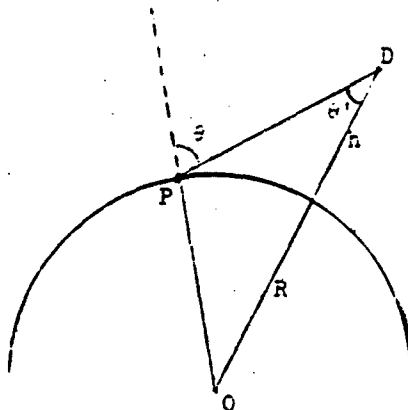


Fig. 7. Detector look angle geometry. The detector D at an altitude  $h$  has a look angle  $\theta'$  to a point P on the earth's surface. The detector zenith angle  $\theta$  is measured from the normal to the surface at P.  $R$  is the radius of the earth with center at O.

Use of the law of sines in triangle OPD leads to

$$\sin \theta = \left(1 + \frac{h}{R}\right) \sin \theta' \quad (31)$$

where

- $\theta$  = detector zenith angle
- $\theta'$  = detector look angle
- $h$  = detector altitude
- $R$  = radius of earth.

Fig. 8 shows a plot of  $\theta$  as a function of  $\theta'$  based on Eq. (31) for various detector altitudes.



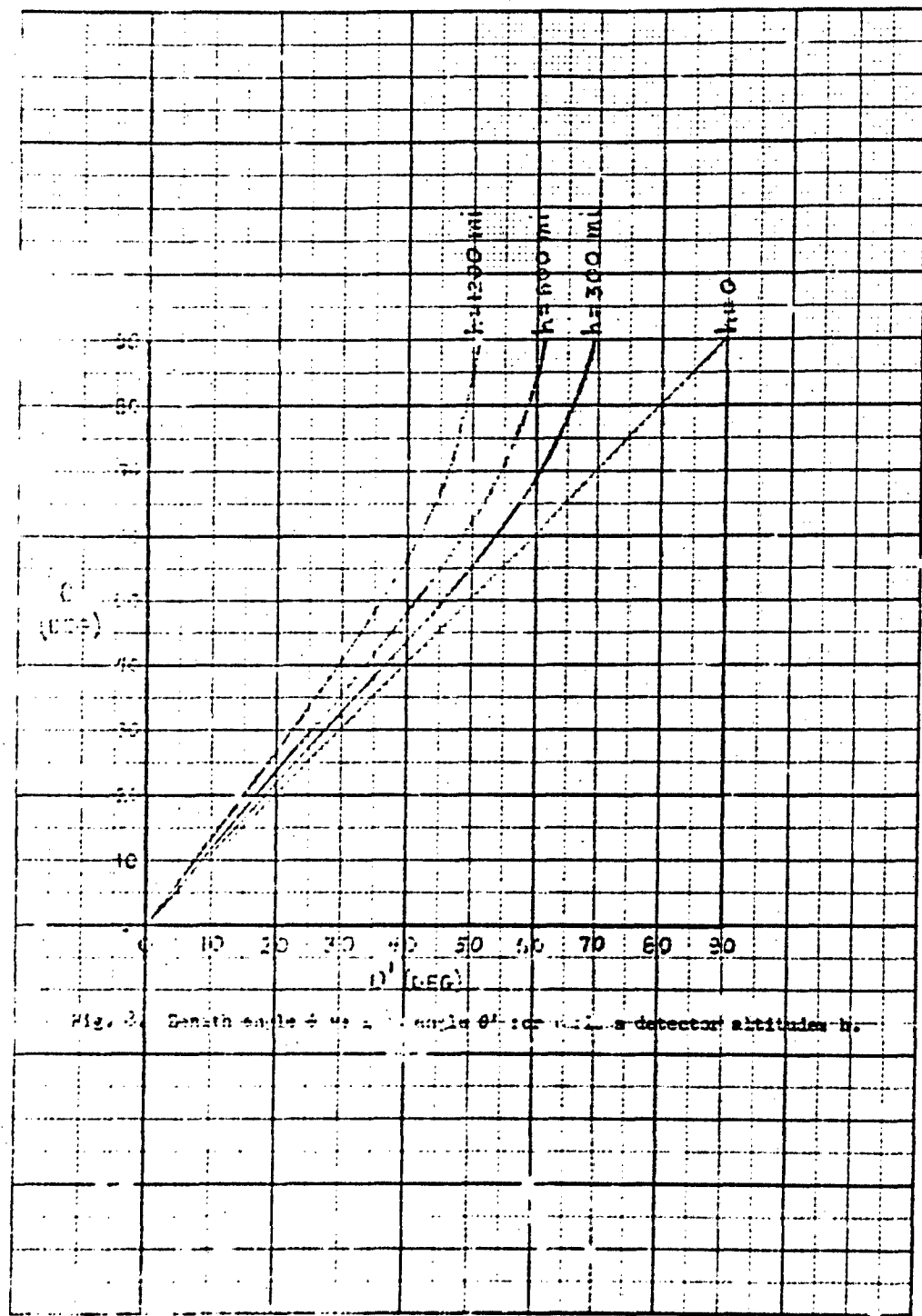


Fig. 3. Zenith angle  $\theta$  vs. angle  $\theta'$  for various detector altitudes  $h$ .

# APPENDIX 4

## LATENT HEAT TRANSFER DUE TO EVAPORATION

If  $Q$  is the amount of heat per unit area required to evaporate a mass  $M$  of water, then

$$Q = \frac{LM}{A}, \quad (32)$$

where

$L$  = latent heat of vaporization of water

$A$  = surface area of the water.

$L$  is the amount of heat required, at a given temperature, to evaporate a unit mass of water. The mass of any substance of uniform density  $\rho$  and volume  $V$  is given simply by the product  $\rho V$ . If we visualize rainfall as being equally distributed over the earth's surface to a height  $h$ , then the volume of water is

$$V = 4\pi R^2 h, \quad (33)$$

where  $R$  is the radius of the earth. Eq. (33) is valid only if  $h$  is very small compared to  $R$ , which is a safe assumption for our case. Therefore,

$$M = 4\pi \rho R^2 h \quad (34)$$

and Eq. (32) becomes

$$Q = \frac{4\pi \rho L R^2 h}{A}. \quad (35)$$

The surface area of the water is

$$A = 4\pi (R + h)^2 \approx 4\pi R^2. \quad (36)$$

Therefore,

$$Q = \rho L h. \quad (37)$$

If it takes a time  $t$  for all the water to evaporate, then the average power per unit area  $W$  required over the time interval  $t$  is

$$W = \frac{Q}{t} = \frac{\rho L h}{t}. \quad (38)$$

For water at 20°C,

$$L = 585 \text{ cal/gm} = 2,450 \text{ joules/gm}$$

$$\rho = 1.$$

Since the global mean rainfall is about 100 cm, the value of  $W$  averaged over a year ( $3.16 \times 10^7$  sec) is  $7.8 \text{ mw/cm}^2$ .

# DISTRIBUTION LIST

<u>To</u>	<u>Copies</u>
Chief Signal Officer, Department of the Army, ATTN: SIGRD-5b Washington 25, D. C.	1
Chief Signal Officer, Department of the Army, ATTN: SIGPD-8b1 Washington 25, D. C.	2
Office of the Assistant Secretary of Defense (Research and Engineer- ing), Technical Library, Room 3E1065, The Pentagon, Washington 25, D. C.	1
Chief, United States Army Security Agency, Arlington Hall Station, ATTN: ACofS, G4 (Technical Library), Arlington 12, Virginia	1
Commanding Officer, U. S. Army Signal Missile Support Agency, ATTN: SIGMS-AJ, White Sands Missile Range, New Mexico	1
Directorate of Intelligence, Headquarters, United States Air Force, ATTN: AFOIN-1b1, Washington 25, D. C.	2
Commander, Rome Air Development Center, ATTN: RA0IL-2, Griffiss Air Force Base, New York	1
Commander, Aeronautical Systems Division, ATTN: ASAPRL, Wright- Patterson Air Force Base, Ohio	1
Commanding General, U. S. Army Electronic Proving Ground, ATTN: Technical Library, Fort Huachuca, Arizona	1
Commander, USAF Security Service, ATTN: Directorate of Systems Engineering (ESD), DCS/Communications-Electronics, San Antonio, Texas	1
Commander in Chief, Strategic Air Command, ATTN: DOCER, Offutt AFB, Nebraska	1
Commander, Air Force Cambridge Research Laboratories, ATTN: CRO, Laurence G. Hanscom Field, Bedford, Massachusetts	2
Chief of Naval Research, Department of the Navy, ATTN: Code 427, Washington 25, D. C.	1
Bureau of Ships Technical Library, ATTN: Code 312, Room 1528 Main Navy Bldg., Washington 25, D. C.	1
Chief, Bureau of Ships, ATTN: Code 45, Department of the Navy, Washington 25, D. C.	1
Director, U. S. Naval Research Laboratory, ATTN: Code 2027, Washington 25, D. C.	1

DISTRIBUTION  
(Contd)

<u>To</u>	<u>Copies</u>
Commanding Officer and Director, U. S. Navy Electronics Laboratory, ATTN: Library, San Diego 52, California	1
Commander, U. S. Naval Ordnance Laboratory, White Oak, Silver Spring, Maryland	1
Director, U. S. Army Engineer Research and Development Laboratories, ATTN: Technical Documents Center, Fort Belvoir, Virginia	1
Commanding Officer, U. S. Army Chemical Warfare Laboratories, ATTN: Technical Library, Bldg. 330, Army Chemical Center, Maryland	1
Commander, Armed Services Technical Information Agency, ATTN: TIPCR, Arlington Hall Station, Arlington 12, Virginia	10
Signal Corps Liaison Officer, Ordnance Tank Automotive Command, U. S. Army Ordnance Arsenal, Detroit, Center Line, Michigan	1
Signal Corps Liaison Officer, Naval Research Laboratory, ATTN: Code 1071, Washington 25, D. C.	1
Signal Corps Liaison Officer, Massachusetts Institute of Technology, 77 Massachusetts Avenue, Bldg. 26, Room 131, Cambridge 39, Massachusetts	1
Commanding General, HQ Ground Electronics Engineering Installation Agency, ATTN: ROZMS, Griffiss Air Force Base, New York	1
Signal Corps Liaison Officer, Lincoln Laboratory, P. O. Box 73, Lexington, Massachusetts	1
Signal Corps Liaison Officer, Rome Air Development Center, ATTN: RAOL, Griffiss Air Force Base, New York	1
USASRDL Liaison Officer, Hq., U. S. Continental Army Command, Fort Monroe, Virginia	1
USASIMA Liaison Engineer, Sig 1 Section, Eighth U. S. Army, APO 301, San Francisco, California	1
Commander, Air Proving Ground Center, ATTN: Adj/Technical Reports Branch, Eglin Air Force Base, Florida	1
Chief, Bureau of Ships, Department of the Navy, ATTN: Code 666B, Washington 25, D. C.	1
Chief of Research and Development, Department of the Army, Washington 25, D. C.	2

DISTRIBUTION  
(Contd)

<u>To</u>	<u>Copies</u>
Signal Corps Liaison Officer, Aeronautical Systems Division, ATTN: ASDL-9, Wright-Patterson Air Force Base, Ohio	2
Commander, Air Force Electronic Systems Division, ATTN: CCRR & CCSD, Laurence G. Hanscom Field, Bedford, Massachusetts	2
AFSC Liaison Office, Naval Air Research & Development Activities Command, Johnsville, Pennsylvania	1
Commanding Officer, USA Signal Electronic Research Unit, P. O. Box 205, Mountain View, California	1
Chief, West Coast Office, U. S. Army Signal Research & Development Laboratory, 75 South Grand Avenue, Bldg. 13, Pasadena 2, California	1
Commanding Officer, U. S. Army Signal Materiel Support Agency, ATTN: SIGFM/ES-ADJ, Fort Monmouth, New Jersey	1
Corps of Engineers Liaison Officer, SIGRA/SL-LNE, Hq, USASRD	1
USASMSA Liaison Office, SIGRA/SL-LNW, Hq, USASRD	1
Marine Corps Liaison Officer, SIGRA/SL-LNR, Hq, USASRD	1
Chief Scientist, SIGRA/SL-CS, Hq, USASRD	1
U. S. CONARC Liaison Officer, SIGRA/SL-LNF, Hq, USASRD	2
Technical Documents Center, USASRD, Evans Area	1
Commanding Officer, U. S. Army Signal Research Activity, Evans Area	1
Chief, Technical Information Division, Hq, USASRD	6
SA File Unit Nr. 1, Hq, USASRD	1
Chief, Reconnaissance Branch Applied Physics Division, SIGRA/SL-SAR, Hq USASRD	30

[illegible]